

IMPROVED PROCEDURE FOR DESIGN AND EVALUATION OF STRUCTURES: SINGLE-DEGREE-OF-FREEDOM BILINEAR SYSTEMS

B. Chikh¹, L. Moussa², Y. Mehani¹, A. Zerzour², H. Bechtoula¹ and A. Benyoucef²

¹National Center for Applied Research in Earthquake Engineering, CGS
Rue Kaddour Rahim Prolongée, Hussein Dey, Alger
Cheikhpsd@gmail.com

²High National School of Public Works, ENSTP
BP. 32, Garidi I, Vieux Kouba 16051, Algiers, Algeria

Keywords: Improved Procedure, Design, Evaluation, Bilinear System.

Abstract. *Current seismic codes require from the seismically designed structures to be capable to withstand inelastic deformations. Many studies dealt with the development of different inelastic spectra with the aim to simplify the evaluation of inelastic deformations and performance of structures. Recently, the concept of inelastic spectra has been adopted in the global scheme of the performance-based seismic design through capacity-spectrum methods. In this paper an improved procedure, applicable to evaluation and design of structures has been developed and illustrated by examples. This procedure uses inelastic spectra and gives peak responses consistent with those obtained when using the nonlinear time history analysis. The idea consists of solving the differential equation of motion for an increased horizontal displacement of the system. Also, is developed the modified Procedure A of ATC 40 for estimating the seismic deformation of SDOF systems.*

1 INTRODUCTION

Since the development of the Capacity-Spectrum Method (CSM) (Freeman et al. 1975) [1], many response spectra have been proposed to replace the conventional elastic spectra in order to achieve accurate evaluation of the inelastic response of structures.

Recently, Miranda (2000) [11] proposed procedures based on displacement modification factors in which the maximum inelastic displacement demand of multi-degree of freedom (MDOF) system is estimated by applying certain displacement modification factors to maximum deformation of equivalent SDOF system having the same lateral stiffness and damping coefficient as that of MDOF system. In another study, Miranda and Ruiz-Garcia (2002) evaluated six possible alternative methods to estimate the maximum inelastic deformations of SDOF systems [2]. The evaluated methods estimate the maximum inelastic deformation using functions of displacement ductility factor to compute equivalent periods and equivalent damping ratios (Rosenblueth and Herrera 1964, Gulkan and Sozen 1974, Iwan 1980, Kowalsky 1994), or to compute displacement modification factors (Newmark and Hall 1982, Miranda 2000) [11]. The study aimed at evaluating the accuracy of approximate methods for the preliminary design of structures. Later, Akkar and Miranda (2002) conducted a statistical evaluation of five of the above methods. The study showed that for periods longer than 1 second all methods produce relatively good results. In the short period region, equivalent linear methods proposed by Iwan and Guyader and the one proposed by Kowalsky tend to overestimate deformation demands [8]. The errors produced by any of the evaluated approximate methods can be relatively larger, particularly for lateral strength ratios larger than four.

The capacity-spectrum method gives an overall view of the inelastic behavior of structures subjected to ground motions. However, to be as more accurate as possible it requires a realistic capacity curve for the structure that is in accordance with its dynamic behavior when subjected to the design earthquake. Many refinements and corrections have been made to the pushover analysis to make it in accordance with the nonlinear time history analysis. For instance, the adaptive pushover analysis (A. S. Elnashai 2001, among others) actually represents the best choice.

Based on the deficiencies in ATC-40 [1] procedures (Applied Technology Council 1996), Chopra and Goel (1999) proposed an improved Capacity-Demand-Diagram method that uses the constant-ductility design spectrum [3]. Their method has been evaluated using SDOF elastoplastic systems, and to retain the attraction of the graphical implementation of the ATC-40 procedures (A and B) Chopra and Goel developed an alternative graphical implementation of their improved method.

In this paper, we first present the development of the ductility demand response spectrum. Based on the inaccuracy of ATC-40 [1] procedures and the need to a graphical approach for the seismic design of structures, an improved procedure were proposed and investigated in this paper.

2 ATC-40 PROCEDURES

ATC-40 [1] specifies three different procedures of the Capacity Spectrum Method (CSM) to estimate the earthquake-induced deformation and finding the performance point, all based on the same principles, but differing in implementation. Procedures A and B are analytical and amenable to computer implementation, whereas procedure C is graphical and most suited for hand analysis. Designed to be the most direct application of the methodology, Procedure A is suggested to be the best of the three procedures [1]. The Capacity Spectrum Method (CSM) compares the capacity of a structure to resist lateral forces to the demands of earthquake response spectra in a graphical presentation that allows a visual evaluation of how the

structure will perform when subjected to earthquake ground motion. The method is easily understandable and generally consistent with other methods that take into account the nonlinear behavior of structures subjected to strong motion earthquake ground movements [5].

The procedure can be summarized by the following :

- Capacity curve: Estimate or calculate the capacity curve in terms of roof displacement x , and base shear, V_b (i.e. total lateral force at base).
- Dynamic characteristics: Estimate or calculate modal vibrational characteristics such as periods of vibration, mode shapes, modal participation factors, and effective modal mass ratios.
- Capacity Spectrum: Convert the V_b vs x capacity curve to a S_a vs S_d capacity spectrum by use of dynamic characteristics..
- Response Spectra: Obtain or calculate response spectra for several levels of damping, including the 5-percent damped spectrum.
- Graphical Solution: Plot capacity spectrum and family of damped response spectra on an ADRS format (i.e. S_a vs S_d coordinates with period T lines radiating from origin). The intersection of the capacity spectrum with the appropriately damped response spectrum represents the estimated demands of the earthquake on the structure.

3 IMPROVED PROCEDURE

A relatively simple method for determining the seismic demands of structures is presented. It combines the Pushover analysis of a single-degree-of-freedom (SDOF) bilinear model shown in figure (1), with a new inelastic response spectrum [2]. This spectrum formulated in the ductility demand – period format are applied. This feature represents the major difference with respect to the capacity spectrum method. Moreover, seismic demand can be obtained without iteration. The differences between the proposed method and the capacity spectrum method are discussed, and some examples are processed to check this difference.

3.1 Capacity curve

Using a Pushover analysis, a characteristic nonlinear force-displacement relationship of the SDOF bilinear system can be determined. The selection of an appropriate lateral load distribution is an important step within the Pushover analysis. Once you done Pushover analysis, the curve is characterized by some parameters. These features will be used for the construction of the demand diagram we will be see in the next step.

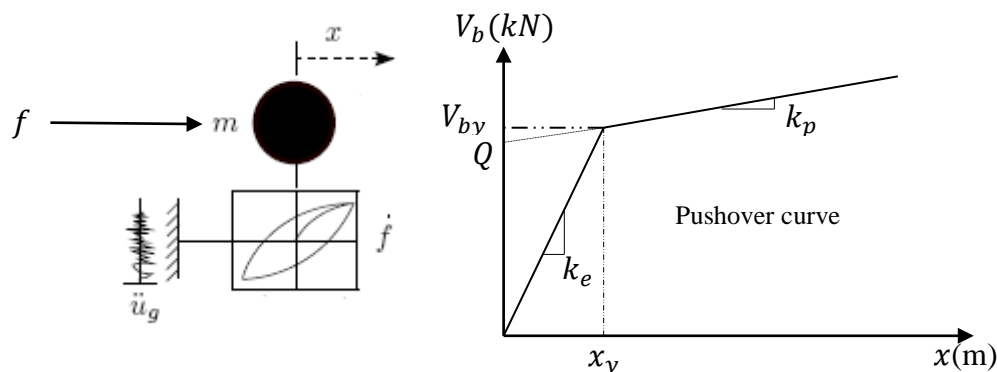


Figure 1: Capacity curve of a (SDOF) bilinear system .

3.2 Seismic demand

The seismic demand for the SDOF bilinear system can be determined by using the following procedure. Both the demand spectra and the capacity diagram are not plotted in the same graph.

3.2.1 Equation of motion in terms of ductility

Considering an inelastic single-degree of freedom system, its motion when subjected to an earthquake ground motion is governed by the following equation:

$$m\ddot{x} + c\dot{x} + f(x, \dot{x}) = -m\ddot{u}_g(t) \quad (1)$$

Where, m , c and f represent the mass, damping, and the resisting force of the system, respectively, $\ddot{u}_g(t)$ denotes the earthquake acceleration. The resisting force f is defined as the sum of a linear part and a hysteretic part:

$$f = k_p x + Qz \quad (2)$$

In the above, k_p is the postyield stiffness, Q is the yield strength, and z represents the dimensionless variable that characterizes the Bouc-Wen model of hysteresis [17], it is given by:

$$\dot{z} = \frac{\dot{x}}{x_y} \left[A - |z|^n (\gamma \operatorname{sgn}(\dot{x}z) + \beta) \right] \quad (3)$$

In the above equation, x_y is the yield displacement, A , η , γ , and β are parameters that control the shape of the hysteresis loop. Material degrading is not considered in this study. However, to accommodate material degradation in the hysteresis model, the Baber-Noori (1985) version of the Bouc-Wen model may be used.

Substituting Eq. (2) into Eq. (1) and dividing by m yields :

$$\ddot{x} + 2\xi\omega\dot{x} + \frac{k_p}{m}x + \frac{Q}{m}z = -\ddot{u}_g(t) \quad (4)$$

Or simply:

$$\ddot{x} + 2\xi\omega\dot{x} + \alpha\omega^2x + qgz = -\ddot{u}_g(t) \quad (5)$$

In which ξ , ω , α , and q represent the damping ratio, circular frequency, post-to-preyield stiffness ratio, and the yield strength coefficient (defined as yield strength divided by the system weight $W : W = mg$, g stands for the gravity), respectively.

Equation 5 is solved for a single ground acceleration (see Fig. 2a) to obtain the deformation history $x(t)$ (Fig. 2b). Also shown is the yielding history through $z(t)$ (Fig. 2c) and the variation of the system force coefficient f/w with deformation (Fig. 2d).

Next, Eq. (5) is rewritten in terms of displacement ductility factor, μ . Substituting: $x = x_y\mu$, $\dot{x} = x_y\dot{\mu}$, and $\ddot{x} = x_y\ddot{\mu}$, in Eq. (5) and dividing by x_y gives [2]:

$$\ddot{\mu} + 2\xi\omega\dot{\mu} + \alpha\omega^2\mu + \frac{qgz}{x_y} = -\frac{1}{x_y}\ddot{u}_g(t) \quad (6)$$

By doing the same to the dimensionless variable z , Eq. (3) may be expressed in terms of $\dot{\mu}$ as:

$$\dot{z} = \dot{\mu} \left[A - |z|^n (\gamma \operatorname{sgn}(\dot{x}z) + \beta) \right] \quad (7)$$

The term $\frac{qgz}{x_y}$ in Eq. (6) is rewritten as:

$$\frac{qg}{x_y} = \omega^2(1 - \alpha) \quad (8)$$

Solving Eq. (8) for x_y yields:

$$x_y = \frac{qg}{\omega^2(1 - \alpha)} \quad (9)$$

Substituting Eq. (8) and Eq. (9) into Eq. (6) gives [2]:

$$\ddot{\mu} + 2\xi\omega\dot{\mu} + \alpha\omega^2\mu + \omega^2(1 - \alpha)z = -\frac{\omega^2(1 - \alpha)}{qg}\ddot{u}_g(t) \quad (10)$$

We observe from Eq. (10) that for a given ground acceleration, $\mu(t)$ depends on ξ, ω, α , and q .

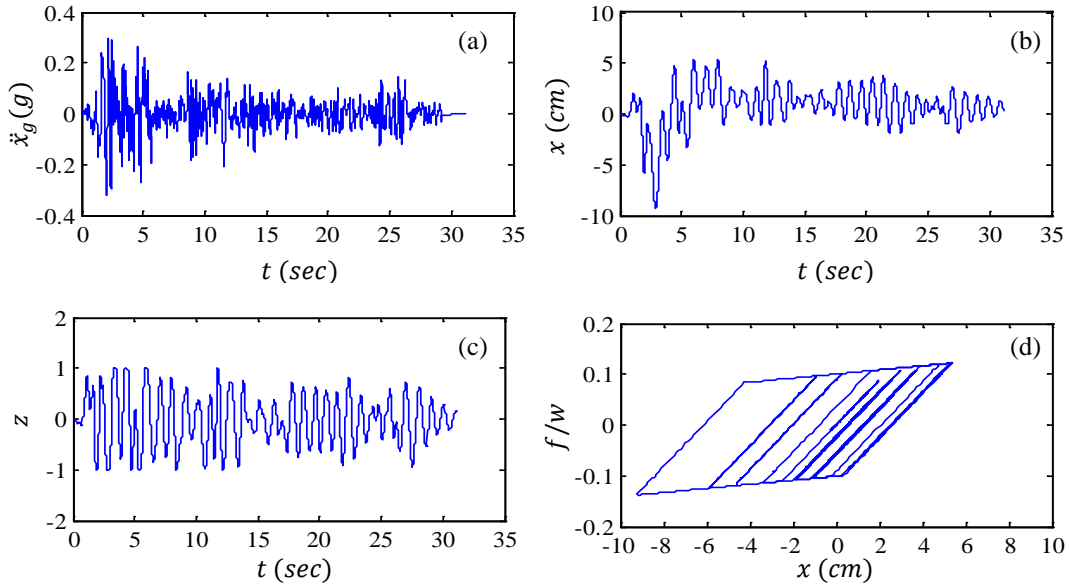


Figure 2 : (a) Strong component of El Centro 1940 ground motion, (b) system deformation, (c) yield function $z(t)$, and (d) force-deformation relation. System parameters are $x_y = 2.5\text{ cm}$, $T = 1.0\text{ sec}$, $k_e = 17488.9\text{ N/cm}$ and $\alpha = 10\%$.

3.2.2 System controlling parameters and normalization

To obtain meaningful system response to an ensemble of ground motions, the system yield strength coefficient has to be defined relative to the intensity of individual ground motions. Using the parameter η introduced by Mahin and Lin (1983) as [9]:

$$\eta = \frac{qg}{PGA} \quad (11)$$

where, PGA stands for the Peak Ground Acceleration. Incorporating η into Eq. (10) results:

$$\ddot{\mu} + 2\xi\omega\dot{\mu} + \alpha\omega^2\mu + \omega^2(1 - \alpha)z = -\frac{\omega^2(1 - \alpha)}{\eta}\overline{\ddot{u}}_g(t) \quad (12)$$

in which, $\overline{\ddot{u}}_g(t)$ represents the ground acceleration normalized with respect to the PGA:

$$\overline{\ddot{u}}_g(t) = \frac{\ddot{u}_g(t)}{PGA} \quad (13)$$

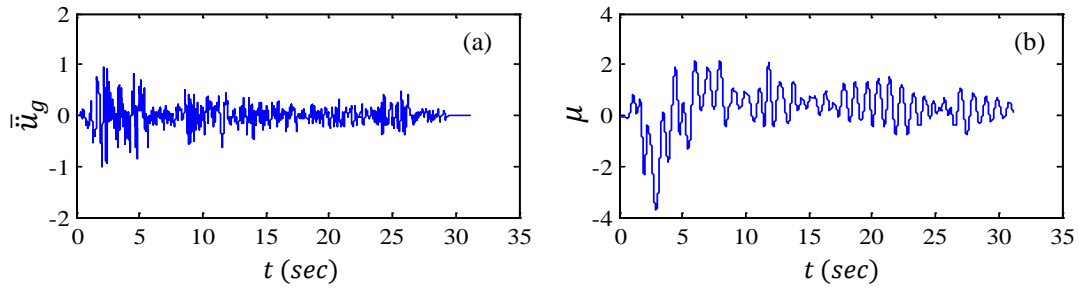


Figure 3: (a) Strong component of normalized ground acceleration of El Centro 1940 and (b) ductility demand μ for a system with $x_y = 2.5$ cm, and $\eta = 0.25$.

Figure 3. demonstrates the normalized ground acceleration history of the strong component of El Centro 1940 and the resulting ductility demand, in contrast to Fig. 2 that presented their unnormalized counterparts.

The ground acceleration has been normalized such that its value varies from -1 to 1. Eq. (12) implies that for a given inelastic system, if α and η are fixed, the intensity of the ground motion has no effect on the peak normalized deformation, μ . This permits the construction of the ductility response spectrum for an ensemble of ground motions with common frequency content but variable intensity.

3.2.3 Constant – η ductility response spectrum

The procedure to construct the ductility response spectrum for inelastic systems corresponding to specified levels of normalized yield strength η , is summarized in the following steps [2]

- Define the ground motion $\ddot{u}_g(t)$;
- Select and fix the damping ratio ξ and the post-to-preyield stiffness ratio α ($\alpha = 0$ for elastoplastic system) for which the spectrum is to be plotted;
- Specify a value for η ;
- Select a value for elastic period T ;
- Determine the ductility response $\mu(t)$ of the system with T, ξ , and α equal to the values selected by solving Eq. (12) along with Eq. (7). From $\mu(t)$ determine the peak ductility factor μ ;
- Repeat steps 4 and 5 for a range of T , resulting in the spectrum values for the η value specified in step 3;
- Repeat steps 3 to 6 for several values of η .

Given the excitation and the properties T, ξ, α , and η of an inelastic SDOF system, it is desired to determine the peak deformation, x_m . The yield displacement of the system is derived from Eq. (9) and Eq. (11) as follows:

$$x_y = \frac{\eta}{\omega^2(1-\alpha)} PGA \quad (14)$$

The value of the ductility factor is read from the spectrum developed by the above procedure and multiplied by x_y to obtain the peak deformation, x_m . The DDRS is constructed also for El Centro 1940 ground motion (N/S) component (PGA=0.32g, PGV=36.14 cm/sec, and PGD=21.34cm) and is shown in figure 4.

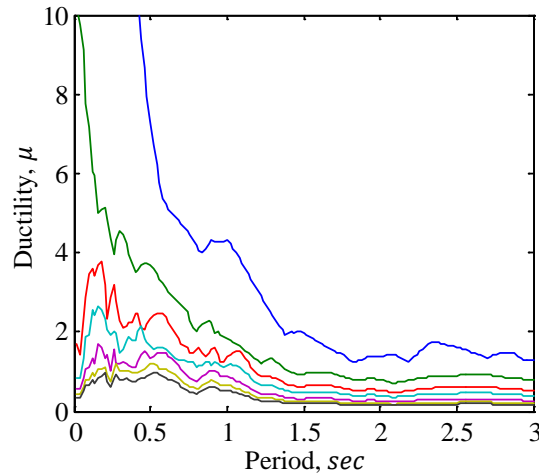


Figure 4: DDRS for inelastic system computed for El Centro 1940 (N/S) component ($\eta = 0.25, 0.5, 0.75, 1, 1.5, 2, 2.5$ from top line to bottom line).

4 APPLICATIONS

It is desired to analyze some examples subjected to the El Centro 1940 north-south component, each system has the properties shown in the table 1. Considered are two values of T : 0.5s in the acceleration sensitive spectral region and 1s in the velocity-sensitive region, and two levels of yield strength; $\zeta=5\%$ for all systems.

system	$m(kg)$	$k_e(N/cm)$	$k_p(N/cm)$	$Q(N)$	$x_y(cm)$
1	1.86	293.72	14.68	290.19	1.04
2				435.29	1.56
3		90.65	4.53	290.23	3.37
4				435.77	5.06

Table 1 Characteristics of inelastic systems.

The results obtained from the nonlinear dynamic analysis (NL-THA) of the systems are summarized in table 2 with the parameter η , which has been calculated by the equation (11).

Systems Properties						(NL-THA)	
system	$T(s)$	$\alpha(\%)$	η	q	$x_y(cm)$	μ	$x_m(cm)$
1	0.5	5%	0.5	0.16	1.04	3.93	4.08
2			0.75	0.24	1.56	2.68	4.18
3	0.9	5%	0.5	0.16	3.37	2.28	7.68
4			0.75	0.24	5.06	1.79	9.05

Table 2 Properties of systems and their responses due to El Centro 1940.

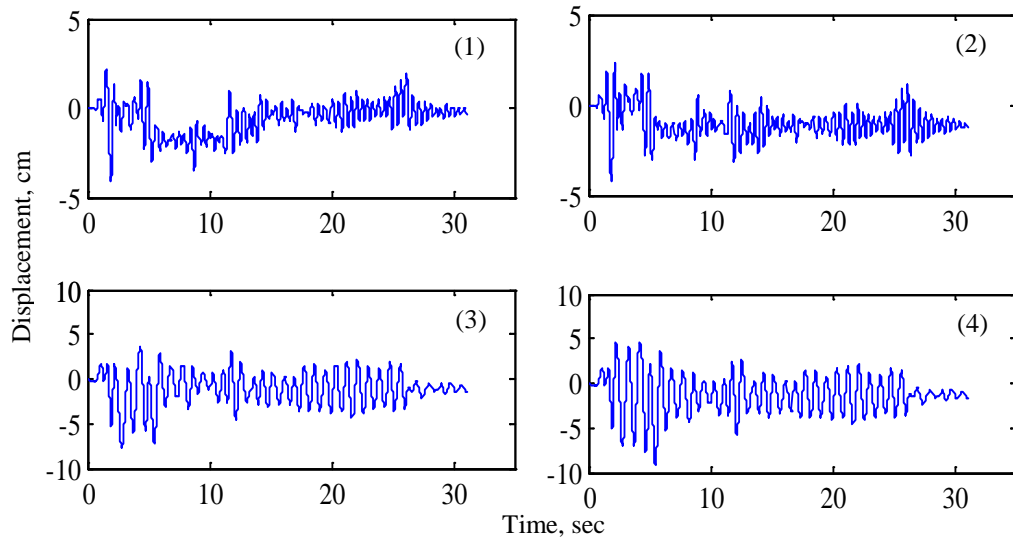


Figure 5: Dynamic nonlinear results of the four systems.

The CSM (Procedure A) is used to compute the earthquake-induced deformation of the four example systems listed in Table 1. Implementation details are presented next for selected systems and final results for all systems in table 3 and figure 6.

system	$D_p(cm)$	$A_p(g)$	μ	$\hat{\xi}(\%)$	Erreur (%) < 5%
1	3.59	0.18	2.91	29.72	0.16
2	3.61	0.26	1.71	22.82	0.25
3	7.83	0.17	1.10	9.0	0.52
4	Divergence				

Table 3: Results from ATC-40 Procedure A analysis of four systems for El Centro (1940) ground motion.

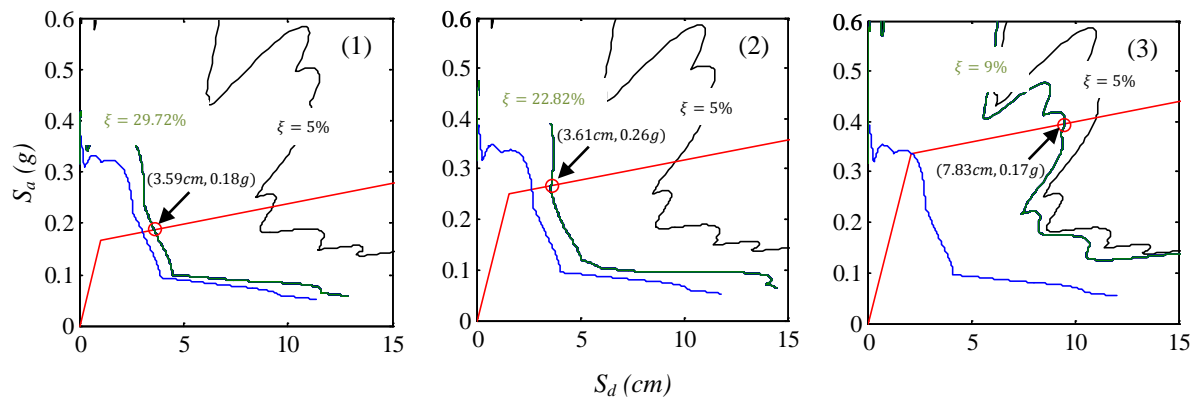


Figure 6: Application of ATC-40 Procedure A to System 1, 2 and 3 for elastic design spectrum - iterative procedure.

The period T and the properties α and η of an inelastic SDOF system are used to compute the ductility and the inelastic displacement of systems by the DDRS spectra. The results obtained from the DDRS of the systems are summarized in table 4.

System	Displacement (cm)			Errors (%)	
	ATC40	DDRS	NL-RHA	ATC40	DDRS
1	3.59	4.08	4.08	12.01	0.0
2	3.61	4.18	4.18	13.64	0.0
3	7.83	7.68	7.68	-02.01	0.0
4	-----	9.05	9.05	-----	0.0

Table 4 Comparison of results obtained by DDRS and CSM.

It is clear from table 4 that the peak response of DDRS is equal to that obtained by the non-linear dynamic (NL-THA) "exact" analysis. Therefore, the DDRS can be considered as an attractive tool since it leads to meaningful and accurate results.

5 CONCLUSION

An improved direct procedure for seismic demands of SDOF bilinear system has been developed and its accuracy was verified by examples, and a response spectrum, called DDRS, has been developed and its applicability was tested for the selected examples. This investigation led to the following conclusions:

- The efficiency of the DDRS is evident; the designer needs only to have the DDRS for the design earthquake (s) to determine peak response of any structure, namely, base displacement and base shear.
- This method is applicable to a variety of uses such as a rapid evaluation technique for a large inventory of buildings, a design verification procedure for new construction, an evaluation procedure for an existing structure to identify damage states.
- Based on this study the ATC-40 Procedure A did not converge for the fourth system analyzed. It converged in many cases but not to the exact deformation determined by nonlinear response history analysis of the inelastic system, nor to the value determined from the DDRS inelastic response spectrum.
- The ductility demand is given by the direct estimation where the ductility calculated from the DDRS diagram matches the value associated with the period of the system. This method gives the deformation value consistent with the selected DDRS inelastic response spectrum, while retaining the attraction of graphical implementation of the ATC-40 methods.

6 REFERENCES

- [1] Applied Technology Council. 1996, "Seismic evaluation and retrofit of concrete buildings", *Report ATC 40*.
- [2] Chikh B., Moussa L., eT Zerzour A, 2012. "Ductility and Inelastic Deformation Demands of Structures", Paper ID: *Structural Engineering and Mechanics* 17289C. Vol. 42, No. 5, June10, 2012. Techno Press P.O. Box 33, Yuseong-gu Daejeon 305-600 KOREA.

-
- [3] Chopra, A. K. and Goel, R. K. (1999), "Capacity-demand-diagrams based on inelastic design spectrum", *Earthq. Spec.*, 15(4), 637-656.
 - [4] 9-Fajfar, P. (1999), "Capacity spectrum method based on inelastic demand spectra", *Earthq. Eng. Struct. Dyn.*, 28(9), 979-993.
 - [5] Freeman, S. A. Nicoletti, J. P. and Tyrell, J. V. (1975), "Evaluation of existing buildings for seismic risk-a case study of Puget Sound Naval Shipyard, Bremerton, Washington", *Proceedings of 1st U.S. National Conference on Earthquake Engineering*, Earthquake Engineering Research Institute, Berkeley, 113-122.
 - [6] Güllkan, P. and Sözen, M. (1974), "Inelastic response of reinforced concrete structures to earthquake motions", *ACI J.*, 71(12), 604-610.
 - [7] Ibarra, L. F. (2003), "Global collapses of frame structures under seismic excitations", Ph.D. Thesis, *Department of Civil and Environmental Engineering, Stanford University*, Stanford, California.
 - [8] Iwan, W. D., (1980), "Estimating inelastic spectra from elastic spectra", *Earthq.Eng. Struct.Dyn.*, 8(4), 375-388.
 - [9] Mahin, S. A. Lin, J. (1983), "Construction of inelastic response spectra for single-degree-of-freedom systems. Computer program and applications", *Report No. UCB/EERC-83/17, University of California*, Berkeley.
 - [10] Miranda, E. (1992), "Nonlinear response spectra for earthquake resistant design", *Proceedings of the Tenth World Conference on Earthquake Engineering*, Balkema, Rotterdam, 5835-5840.
 - [11] Miranda, E. (2000), "Inelastic displacement ratios for structures on firm sites", *J. Struct. Eng.*, 126(10), 1150-1159.
 - [12] Miranda, E. (2001), "Estimation of inelastic deformation demands of SDOF systems", *J. Struct. Eng.*, 127(9), 1005-1012.
 - [13] Moussa. L, 2009 "Base Isolated Buildings Parametric Analysis and Design Guidelines", Thesis in Civil Engineering, *Technical university of civil engineering, Bucharest*, September 2009.
 - [14] Nassar, A. and Krawinkler, H. (1991), "Seismic demands for SDOF and MDOF systems", John A. Blume *Earthquake Engineering Center*, Report 95, Dept. of Civil Engineering, Stanford University.
 - [15] Newmark, N. M. and Hall, W. J. (1982), "Earthquake spectra and design", *Earthquake Engineering Research Institute*, Berkeley, California.
 - [16] Ruiz-Garcia, J. and Miranda, E. (2003), "Inelastic displacement ratios for evaluation of existing structures", *Earthq.Eng. Struct.Dyn.*, 32(8), 1237-1258.
 - [17] Wen, Y. K. (1976), "Method for random vibration of hysteretic systems", *J. Eng. Mech.*, 102(2), 249-263.